Effect of Pressure on the Quadrupole Interaction in Iron-Fluorine Compounds*

C. W. CHRISTOE AND H. G. DRICKAMER
Department of Physics, Department of Chemistry and Chemical Engineering, and Materials Research Laboratory, University of Illinois, Urbana, Illinois 61801
(Received 18 August 1969)

The interaction between the nuclear quadrupole moment and the electric field gradient at the nucleus for Fe(III) in K_3FeF_6, Na_3FeF_6, and $(NH_4)_3FeF_6$ has been measured to 170-kbar pressure. The quadrupole splitting increases markedly with increasing pressure. Calculations are presented for both a point-charge and a covalent model of K_3FeF_6. In both cases a relatively small change in local symmetry with presure will account for the results. The amount of covalency appears to be appreciable. Similar calculations are made for FeF_2 using previously published quadrupole-splitting data plus x-ray measurements of the c and a axes as a function of pressure. The observed decrease in quadrupole splitting can be accounted for qualitatively. The effect of covalency is negligible.

INTRODUCTION

IN this paper we discuss the effect of pressure (interatomic distance) on the interaction between the nuclear quadrupole moment and the electric field gradient at the nucleus for compounds of Fe(III) and Fe(II) with F^- ligands. New Mössbauer resonance data are presented for K_3FeF_6, Na_3FeF_6, and $(NH_4)_3FeF_6$, along with an analysis of the first compound. Previously published data[1] for FeF_2 are also analyzed in terms of new x-ray data.

The ferric compounds were synthesized from iron enriched to 90% in Fe^{57}. The high-pressure Mössbauer resonance techniques have been presented in detail elsewhere.[2]

FERRIC COMPOUNDS

As mentioned above, the chief concern in this work is with the quadrupole splitting. Before discussing this in detail, two other observations should be mentioned. For these compounds there was observed a small decrease in isomer shift (center of gravity of the spectrum) with increasing pressure (0.02–0.05 mm/sec in 150 kbar), corresponding to a small increase in electron density at the iron nucleus. This is similar in direction but smaller in magnitude than that observed for a variety of other iron compounds.[1] Since the increase in s electron density is usually associated with a spreading of the $3d$ orbitals due to interaction with the ligands, it is not surprising that the change is small for F^- ligands. For a wide variety of compounds it has been shown that Fe(III) reduced to Fe(II) with increasing pressure.[3,4] Figures 1(a) and 1(b), giving typical spectra, show that this phenomenon is present in the salts studied here also. However, the conversion never exceeded 20% so that a quantitative discussion is difficult. In any case, the phenomenon is analyzed in detail elsewhere[4] and so will not be discussed further here.

Quadrupole Splitting

The quadrupole splitting as a function of pressure for the ferric salts are presented in Figs. 2 and 3. Since Fe(III) is an S state, in strictly octahedral (or tetrahedral) symmetry no quadrupole splitting would be expected. For all salts of Fe(III) there apparently exist distortions, as all of these compounds exhibit significant quadrupole splitting. As can be seen, the quadrupole splitting increases markedly with increasing pressure; this is a general phenomenon for ferric compounds.[1] Since K_3FeF_6 is the best characterized system we have studied we shall discuss this compound in some detail, with the hope that the ideas will have some general application.

For K_3FeF_6, the $(FeF_6)^{3-}$ complex occupies positions of a face-centered lattice with an $(FeF_6)^{3-}$ at 0 0 0. The potassium occupies two kinds of sites; one type is that of a face-centered lattice intermeshed with that of the $(FeF_6)^{3-}$, but having a K^+ at $\frac{1}{2}$ $\frac{1}{2}$ $\frac{1}{2}$. The other type of potassium site is at the centers of the octants of the $(FeF_6)^{3-}$—or of the K^+-face-centered cell. The unit cell is cubic and its edges define the lattice vectors. Figure 4 portrays the unit cell. The six F^- ions form a slightly distorted octahedron about the Fe(III). These six fluorines lie near, but not exactly along, the lattice vectors. Their locations, relative to the origin at the iron, are given by Bode and Voss[5] as $\pm[(x,y,z);(z,x,y);(y,z,x)]$, where $x=0.21\ a_0$, $y=0.04a_0$, and $z=-0.03a_0$. Figure 5 illustrates the $(FeF_6)^{3-}$ octahedron. The lattice parameter a_0 equals 8.581 Å. The Fe-F distance equals $0.216a_0$ or 1.85 Å for all the fluorines. As indicated in Fig. 5, the F-F distances are not all equal; $A=0.302a_0$ while $B=0.308a_0$. It is convenient to select the axis of highest symmetry of this octahedron, ignoring the rest of the crystal, as the z axis. This axis now passes through the centers of the two equilateral triangles

* This work was supported in part by the U. S. Atomic Energy Commission under Contract No. AT(11-1)-1198.
[1] A. R. Champion, R. W. Vaughan, and H. G. Drickamer, J. Chem. Phys. **47**, 2583 (1967).
[2] P. Debrunner, R. W. Vaughan, A. R. Champion, J. Cohen, J. Moyzis, and H. G. Drickamer, Rev. Sci. Instr. **37**, 1310 (1966).
[3] H. G. Drickamer, R. W. Vaughan, and A. R. Champion, Accts. Chem. Res. **2**, 40 (1969).
[4] H. G. Drickamer, G. K. Lewis, Jr., and S. C. Fung, Science **163**, 885 (1969).
[5] H. Bode and E. Voss, Z. Anorg. Allgem. Chem. **290**, 1 (1957).

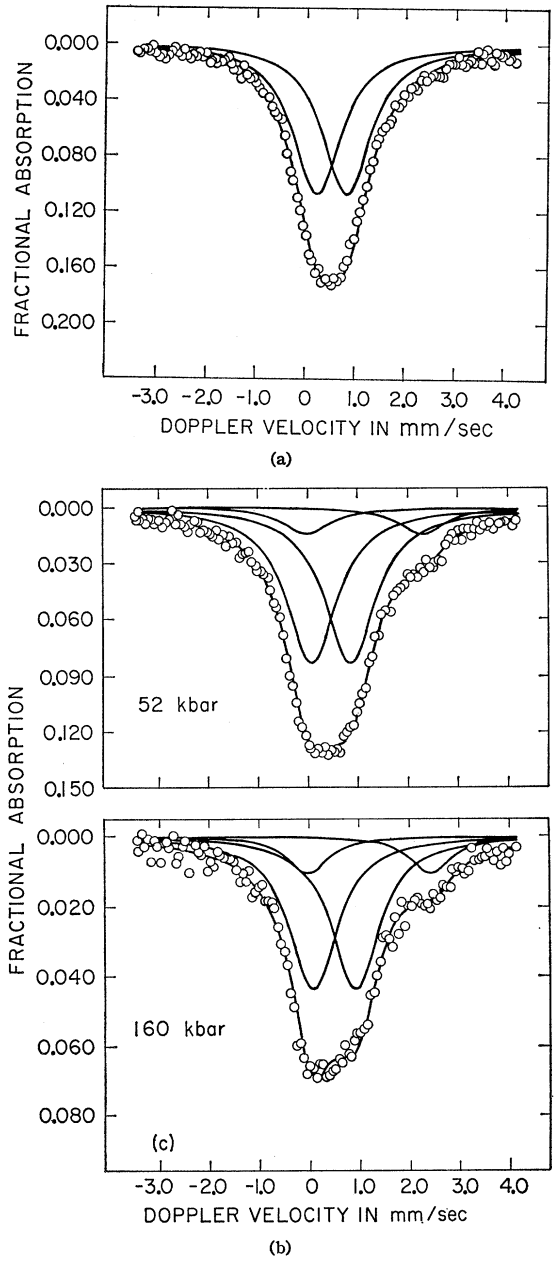

FIG. 1. (a) Spectrum of K_3FeF_6—1 atm.
(b) Spectra of K_3FeF_6 (cont'd.).

(of side A) and the fluorines are distributed in threefold symmetry about it. (See Fig. 6.) If B were equal to A, the octahedron would be regular and the fluorines would lie at what shall be referred to here as the trigonal angle θ_T with respect to the trigonal axis z. θ_T is such that $\cos^2\theta_T=\frac{1}{3}$. As it is, however, the fluorines lie at θ_0 and $\pi-\theta_0$ such that $\cos^2\theta_0=0.347$. Since the azimuthal locations are regular ($\phi_0=0$, $\pm\frac{2}{3}\pi$ if $\theta<\frac{1}{2}\pi$ and $\phi_0=\pi$, $\pm\frac{1}{3}\pi$ if $\theta>\frac{1}{2}\pi$), this is a standard trigonal distortion along an axis which lies near but not quite parallel to the [1 1 1] direction of the crystal. The

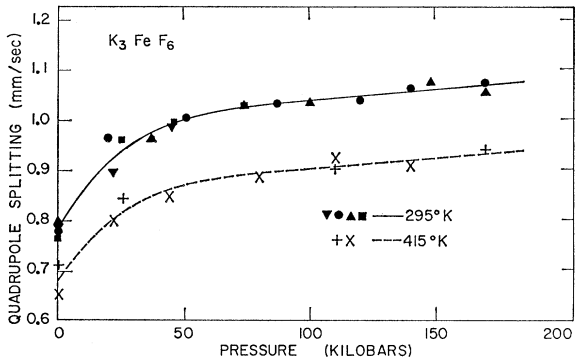

FIG. 2. Quadrupole splitting versus pressure—K_3FeF_6.

x ($\phi=0$) direction is taken to include one of the $\theta<\frac{1}{2}\pi$ fluorine sites.

Point-Charge Model

Since fluorides in general are quite ionic, a point-charge treatment of the quadrupole splitting data might be expected to meet with some success. A point-charge model of high-spin Fe(III) has the five $3d$ electrons distributed according to Hund's rule, that is one in each of the $3d$ orbitals where they constitute a half-filled spherically symmetric shell. Accordingly, the gradient $V_{zz}=q$ is given by q_{field}, plus the core contribution: $q=(1-\gamma_\infty)q_f$, and the asymmetry parameter $(V_{xx}-V_{yy})/V_{zz}=\eta=(1/q)(1-\gamma_\infty)q_f\eta_f=\eta_f$. q_f and η_f can be evaluated for K_3FeF_6 at atmospheric pressure,

$$(q_f)_0=-6(3\cos^2\theta_0-1)/b^3, \tag{1}$$

where b is the Fe-F distance, equal to 1.85 Å or 3.51 a.u.,

$$3\cos^2\theta_0-1=0.0414. \tag{2}$$

(Note that $3\cos^2\theta_T-1=0$.) The above numerical values yield an atmospheric value for the gradient of

$$(q_f)_0=-0.0201 \text{ a.u.} \tag{3}$$

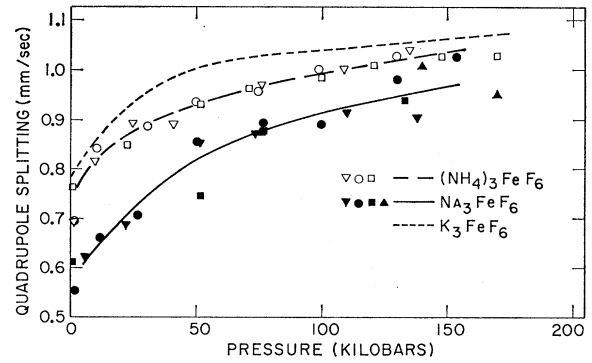

FIG. 3. Quadrupole splitting versus pressure—Na_3FeF_6 and $(NH_4)_3FeF_6$.

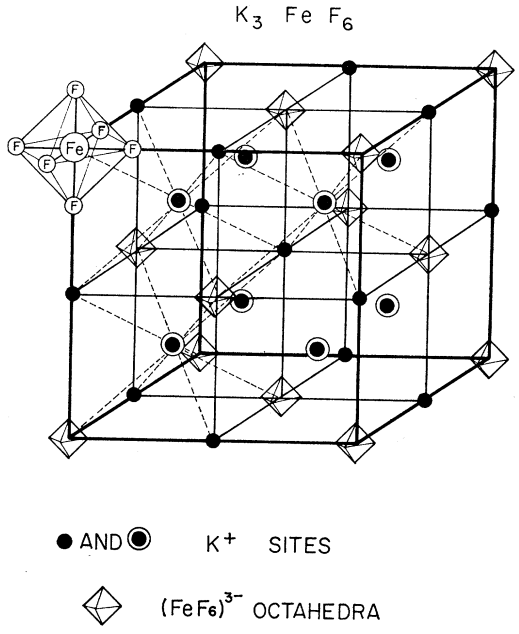

FIG. 4. K_3FeF_6 unit cell.

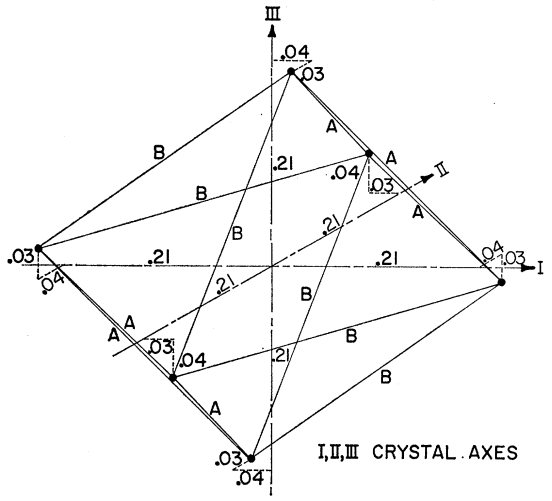

FIG. 5. $(FeF_6)^{-3}$ octahedron in K_3FeF_6.

Because of the threefold symmetry about the z axis, $(\eta_f)_0=0$. The quadrupole splitting is

$$\Delta E=|2E_Q|=(1-\gamma_\infty)Q(0.0201)\text{ a.u.} \quad (4)$$

at atmospheric pressure and room temperature.

Of course, one does not place the greatest of credance in the absolute value of (4), but using Burns's[6] value for Q and either Burns's and Wilkner's[7] value for γ_∞, or Ingalls's value[8] of -10.6 for γ_∞,

$$\Delta E=2.3\text{ or }3.7\times10^{-9}\text{ a.u.}$$
$$=0.65\text{ or }1.05\text{ mm/sec}, \quad (5)$$

which is not unreasonable, as it spans the observed splitting of 0.78 mm/sec. Suppose the factors are chosen so that (4) gives the observed splitting, that is so that $0.78\text{ mm/sec}=6(1-\gamma_\infty)Q(3\cos^2\theta_0-1)/V_0$, where $V_0=b_0^3$ is the volume of the unit cell at atmospheric pressure, then

$$\Delta E=\frac{3\cos^2\theta-1}{V/V_0}(18.82\text{ mm/sec}). \quad (6)$$

One can now calculate from the observed splittings, the pressure dependence of θ required by this model. The results of such a calculation are given in Fig. 7. The values of V/V_0 are taken from the x-ray data of Fanselow.[9]

Recalling that $\theta_T=54.77°$, it is noted that the distortion must first rise with pressure, reach a maximum (minimum θ) at around 50 kbar, and subside. This is because the quadrupole splitting at first grows faster than V_0/V, but above 50 kbar, it rises more slowly with pressure. The atmospheric trigonal distortion is 0.87° and the maximum distortion required by the point-charge model is an additional 0.16° (18%).

Configuration-Interaction Model

Although the point-charge model does not give unacceptable results for the deformations required to produce quadrupole splittings, many authors[10–13] have argued that even for the most ionic ligand, F^-, the point-charge model cannot be physically realistic—most especially in the calculation of energies. Covalency effects have, in fact, been observed directly through the use of nuclear magnetic resonance and electron spin resonance on many iron-series salts[10,14–16] including the cubic salts $KNiF_3$, $KMnF_3$, and K_2NaCrF_6 which demonstrated the presence of unpaired electron density on the fluorine ligands and indicated the presence of covalency. In a series of papers, Shulman and Sugano,[10] Simanek and Sroubek,[11] Watson and Freeman,[12] and

[6] G. Burns, Phys. Rev. **124**, 524 (1961).
[7] G. Burns and E. G. Wilkner, Phys. Rev. **121**, 1955 (1961).
[8] R. Ingalls, Phys. Rev. **128**, 1155 (1962).
[9] D. L. Fanselow, Master's Thesis, University of Illinois, 1969 (unpublished).
[10] S. Sugano and R. G. Shulman, Phys. Rev. **130**, 517 (1963).
[11] E. Šimánek and Z. Šroubek, Phys. Status Solidi **4**, 251 (1964).
[12] R. E. Watson and A. J. Freeman, Phys. Rev. **134**, A1526 (1964).
[13] J. Hubbard, D. E. Rimmer, and F. R. A. Hopgod, Proc. Phys. Soc. (London) **88**, 13 (1966).
[14] R. G. Shulman and K. Knox, Phys. Rev. **119**, 94 (1960).
[15] R. G. Shulman, Phys. Rev. **121**, 125 (1961).
[16] T. P. P. Hall, W. Hayes, R. W. Stevenson, and J. Wilkens, J. Chem. Phys. **38**, 1977 (1963); **39**, 35 (1963).

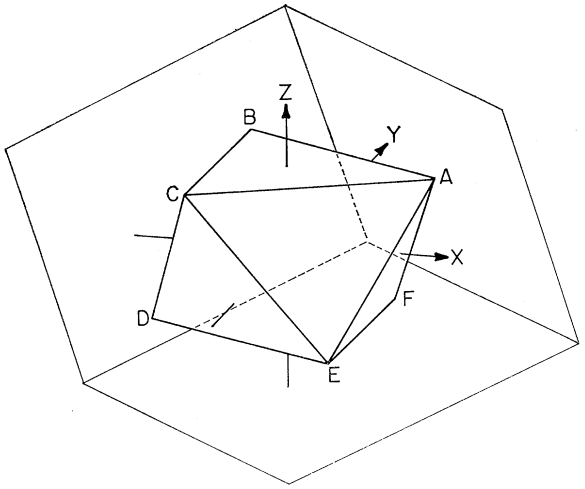

FIG. 6. Choice of axes for $(FeF_6)^{-3}$.

Hubbard, Rimmer, and Hopgood[13] have discussed analytical methods of introducing the proper amount of covalency. In the covalent, configuration-interaction treatment, Hubbard, Rimmer, and Hopgood have defined trial wave functions

$$\Psi=\sum_i \xi_i\Phi_i+\sum_\alpha\sum_{jk} a_{jk}{}^\alpha\Phi_{jk}{}^\alpha, \tag{7}$$

where

$$\Phi_i=A\phi_i{}^{\mathrm{Fe(III)}}\prod_{\beta=1}^{6}\chi_0{}^\beta \tag{8}$$

corresponds to the ith excited configuration of the Fe(III) ion; e.g., a ^4P configuration like $|t_{2g}\uparrow t_{2g}\uparrow e_g\uparrow e_g\downarrow e_g\uparrow\rangle$. Here A is the antisymmetrizing operator, and χ_0 is a fluoride state. The ξ_i are scalar mixing coefficients, expected to be small except for ξ_0, the ground-state coefficient.

$$\Phi_{jk}{}^\alpha=A\phi_j{}^{\mathrm{Fe(II)}}\chi_k{}^\alpha\prod_{\beta\neq\alpha}^{5}\chi_0{}^\beta. \tag{9}$$

$\Phi_j{}^{\mathrm{Fe(II)}}$ is the jth excited Fe(II) configuration and $\chi_k{}^\alpha$ is the kth excited state of the αth fluoride ion. The $\Phi_{jk}{}^\alpha$ represent configurations in which an electron has been transferred from the αth fluoride ion to the iron, whereas the Φ_i represent a transfer of an electron from one iron orbital to another.

It is shown by Hubbard *et al.* that in the event of small overlap,

$$a_{jk}{}^\alpha=-\sum_i\frac{\langle jk\alpha|H-E|i\rangle}{E(jk\alpha)-E}\xi_i, \tag{10}$$

where $E(jk\alpha)=\langle jk\alpha|H|jk\alpha\rangle$ and H is given by

$$H=\sum_\mu\frac{p_\mu{}^2}{2m}+\sum_\mu\Big[V_{\mathrm{Fe}}(\mathbf{r}_\mu)+\sum_{\beta=1}^{6}V_{\mathrm{F}}{}^\beta(\mathbf{r}_\mu)\Big]+\tfrac{1}{2}\sum_{\mu\neq\nu}\frac{e^2}{|\mathbf{r}_\mu-\mathbf{r}_\nu|}, \tag{11}$$

where $V_{\mathrm{Fe}}(\mathbf{r})$ and $V_{\mathrm{F}}{}^\beta(\mathbf{r})$ are the nuclear potentials of the Fe and the βth F respectively, and μ labels all the electrons. E is the energy $\langle\Psi|H|\Psi\rangle$ given by a Ritz variational calculation.

If we assume the functions (7) as zero-order functions, and define h_Q such that

$$\Delta E=\langle\Psi|h_Q|\Psi\rangle=2|E_Q|\,, \tag{12}$$

ΔE, the quadrupole splitting, is given by

$$\langle\Psi|h_Q|\Psi\rangle=\Big\langle\sum_i\xi_i\Phi_i\Big|h_Q\Big|\sum_i\xi_i\Phi_i\Big\rangle+\Big\langle\sum_i\xi_i\Phi_i\Big|h_Q\Big|\sum_\alpha\sum_{j,k}a_{ik}{}^\alpha\Phi_{jk}{}^\alpha\Big\rangle+\text{c.c.}+\Big\langle\sum_\alpha\sum_{jk}a_{jk}{}^\alpha\Phi_{jk}{}^\alpha\Big|h_Q\Big|\sum_\alpha\sum_{jk}a_{jk}{}^\alpha\Phi_{jk}{}^\alpha\Big\rangle. \tag{13}$$

(a) Consider first the terms

$$\Big\langle\sum_i\xi_i\Phi_i\Big|h_Q\Big|\sum_i\xi_i\Phi_i\Big\rangle\quad\text{or}\quad\sum_{i,j}\xi_i\xi_j\langle i|j\rangle. \tag{14}$$

As shown by Hubbard *et al.* ξ_i has a numerator which relates to the transfer potential and a denominator equal to the energy difference between the initial and final states, or between the ground state and the ith excited state. Thus, for K_3FeF_6, the ξ_i which correspond to transfer from one d orbital to another will be of small amplitude since the energy denominator involves spin-pairing energy. It is possible that transfers from E_g levels to $4s$ or $4p$ may be quite important for energy calculations but since neither the s, p nor E_g electrons (when quantized about the threefold axis) produce a field gradient at the nucleus, the Φ_i corresponding to these transfers will not be considered. Thus, the terms (14) are negligible or irrelevant except for $\xi_0\Phi_0$, the ^1S ground-state configuration. For simplicity, we shall take $\xi_0=1$.

(b) Next consider the terms

$$\Big\langle\sum_i\xi_i\Phi_i\Big|h_Q\Big|\sum_\alpha\sum_{j,k}a_{jk}{}^\alpha\Phi_{jk}{}^\alpha\Big\rangle,\quad+\text{complex conjugates}. \tag{15}$$

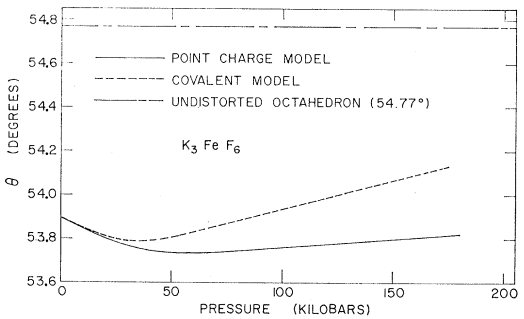

FIG. 7. θ versus pressure—K_3FeF_6.

Equation (10) may now be written as

$$a_{j,k}{}^{\alpha}=-\frac{\langle jk\alpha|H-E|0\rangle}{E(jk\alpha)-E}\xi_0. \tag{16}$$

We see that $a_{jk}{}^{\alpha}$ also contains an energy denominator which is the difference between the energy of the ground state and that of the $\Phi_{jk}{}^{\alpha}$ excited (transfer) configuration. The energy involved in transferring an electron from the fluorine to an iron orbital must be small, since it need not require spin-flip and since, under pressure, it is observed that a number of the iron sites actually reduce by the acquisition of a fluorine electron. (See above.) Group-theoretical arguments, however, dictate the fluorine s and p_σ electrons can transfer only to iron E_g orbitals, while p_π can transfer only to T_{2g}. Again, transfer into an E_g orbital will not affect the quadrupole splitting, thus the a_{jk} of interest are only the $a_{0\pi}$, $a_{+\pi}$, and $a_{-\pi}$, denoting transfer from any of the equivalent fluorines to the $t_{2g}{}^0$, $t_{2g}{}^+$ or $t_{2g}{}^-$ orbitals given by Eqs. (17).

$$\begin{aligned}
&&q\langle r^{-3}\rangle^{-1} \quad &\eta\\
t_{2g}{}^0&=Y_2{}^0, &4/7 \quad &0\\
t_{2g}{}^+&=\frac{\sqrt{2}}{\sqrt{3}}Y_2{}^{-2}+\frac{1}{\sqrt{3}}Y_2{}^1, &-2/7 \quad &0\\
t_{2g}{}^-&=\frac{\sqrt{2}}{\sqrt{3}}Y_2{}^2-\frac{1}{\sqrt{3}}Y_2{}^{-1}, &-2/7 \quad &0.
\end{aligned} \tag{17}$$

Accordingly, we write (9) as

$$\Phi_{j\pi}=A\phi^j\chi_\pi{}^{\alpha}\prod_{\beta\neq\alpha}^{5}\chi_0{}^{\beta}, \quad j=0,+,- \tag{18}$$

where $\Phi^0=|t_{2g}{}^0\uparrow\downarrow t_{2g}{}^+\uparrow t_{2g}{}^-\uparrow\rangle$, etc., while

$$\Phi_0=A\phi_0\prod_{\beta=1}^{6}\chi_0{}^{\beta}, \tag{19}$$

and $\phi_0=|t_{2g}{}^0\uparrow t_{2g}{}^+\uparrow t_{2g}{}^-\uparrow\rangle$.

Equation (15) gives rise to two types of nonzero elements. The first is

$$\sum_{\beta=1}^{5}\langle\chi_0{}^{\beta}|h_Q|\chi_0{}^{\beta}\rangle\langle t_{2g}|p_\pi\rangle.$$

The factor $\langle t_{2g}|p_\pi\rangle$ is not zero since the wave functions have not been properly orthogonalized. This term represents the gradient at the iron site due to a "hole" one of the fluoride sites. One expects this hole to smear out over the six equivalent sites and to produce little net gradient.

The second type is $\langle t_{2g}|h_Q|p_\pi\rangle$ which represents the gradient at the iron site due to charge in the overlap region between the iron and fluorine. Since the overlap is small, as well as nearly symmetrical, this term will be neglected.

(c) Finally, consider the terms

$$\langle\sum_{\alpha}\sum_{j,k}a_{jk}{}^{\alpha}\Phi_{jk}{}^{\alpha}|h_Q|\sum_{\alpha}\sum_{j,k}a_{jk}{}^{\alpha}\Phi_{jk}{}^{\alpha}\rangle$$

or

$$\sum_{\alpha,\alpha'}\sum_{j,j',k,k'}a_{j,k}{}^{\alpha}a_{j',k,}{}^{\alpha'}\langle jk\alpha|h_Q|j'k'\alpha'\rangle. \tag{20}$$

In accord with the foregoing discussion, we shall be interested only in the configurations $\Phi_{0\pi}$, $\Phi_{+\pi}$, and $\Phi_{-\pi}$. Our original zero-order wave functions may now be explicitly written as

$$\Psi=\xi_0\Phi_0+(a_{0\pi}\Phi_{0\pi}+a_{+\pi}\Phi_{+\pi}+a_{-\pi}\Phi_{-\pi}), \tag{21}$$

where only one of each type of transfer is considered since, due to the Pauli principle, only one transfer to any orbital is allowed.

Consider Eq. (16) giving the $a_{jk}{}^{\alpha}$'s. The numerator of this expression is equivalent to

$$\begin{aligned}
&(\langle 0|H-E|0\rangle+\langle+|H-E|+\rangle+\langle-|H-E|-\rangle\\
&\quad+\textstyle\sum_\beta\langle\beta|H-E|\beta\rangle)\langle j|\pi\rangle+\langle j|H-E|\pi\rangle,\\
&\qquad\qquad j=0,+,-.
\end{aligned} \tag{22}$$

The first term in (22) is proportional to the $t_{2g}-p_\pi$ overlap integral, and we may consider the coefficient constant in first order. The second term is a sum of $\langle t_{2g}|H|p_\pi\rangle$ and $E\langle t_{2g}|p_\pi\rangle$, the latter of which is also proportional to the overlap. $\langle t_{2g}|H|p_\pi\rangle$ represents the matrix element for transfer from the p_π orbital to the t_{2g}. This term may be expected to vary with pressure in some complicated manner. However, it is physically reasonable that the variation of the interaction should be monotonic with changes in the overlap. For the purposes of this treatment we shall consider, in first order, $\langle t_{2g}|H|p_\pi\rangle$ as linear in $\langle t_{2g}|p_\pi\rangle$. Within this approximation, the numerator of $a_{j\pi}{}^{\alpha}$ may be considered to be proportional to the $t_{2g}-p_\pi$ overlap integral. This overlap has been evaluated after the method of Mullikan *et al.*[17] with the variation of interatomic distance taken from Fanselow's compressibility data.[9] The numerator of a_{jk} is thus $A\langle d|p\rangle_\pi$ where A is a constant.

The denominator of (16) is dependent upon the energy of the particular t_{2g} to which the transfer is occurring. If the polar location of the fluorides is described as $\cos^2\theta=\frac{1}{3}+\lambda$, the resulting crystal-field potential can be written as

$$V+V_0+W\lambda+\text{terms of order }\lambda^2\text{ and higher}, \tag{23}$$

where V_0 is the octahedral field and $W\lambda$ is a term proportional to the trigonal distortion. W contains $Y_2{}^0$ as well as $Y_4{}^0$. The T_{2g} functions are thus split into a singlet $t_{2g}{}^0$ and a doublet $t_{2g}{}^{\pm}$. If the first-order matrix elements are directly evaluated, it turns out that the

[17] R. S. Mullikan, C. A. Rieke, D. Orloff, and H. Orloff, J. Chem. Phys. **17**, 1248 (1949).

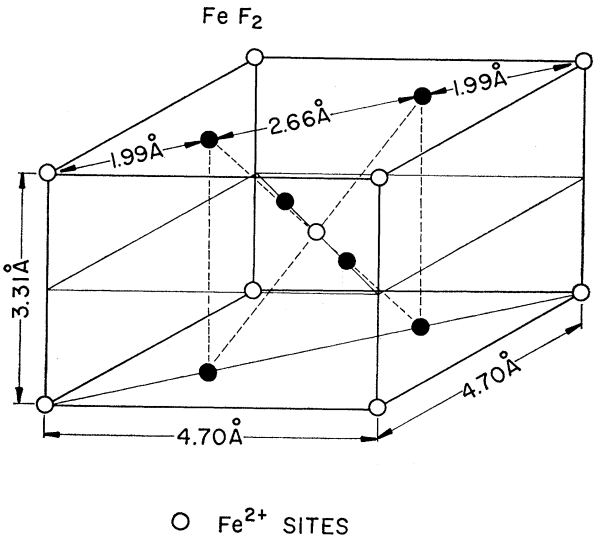

FIG. 8. FeF_2 unit cell.

energy splitting among the T_{2g} levels is $3h\lambda$, where

$$h=\frac{9}{7}Z\frac{\langle r^2\rangle}{b^3}-\frac{5}{7}Z\frac{\langle r^4\rangle}{b^5},$$

and b is again the iron-fluorine distance, and if the denominator of $a_{0\pi}$ is B, then that of $a_{+\pi}$ and $a_{-\pi}$ is $B+3h\lambda$. Equation (13) now appears as[18]

$$\langle\Psi|h_Q|\Psi\rangle=A^2|\langle d|p\rangle|^2\left[\frac{1}{B}\langle\Phi_{0\pi}|h_Q|\Phi_{0\pi}\rangle+\frac{1}{B+3h\lambda}\times(\langle\Phi_{+\pi}|h_Q|\Phi_{+\pi}\rangle+\langle\Phi_{-\pi}|h_Q|\Phi_{-\pi}\rangle)\right]. \quad (24)$$

Let us now take as an example

$$\langle\Phi_{+\pi}|h_Q|\Phi_{+\pi}\rangle=\langle 0|h_Q|0\rangle+2\langle+|h_Q|+\rangle+\langle-|h_Q|-\rangle+\langle\pi|h_Q|\pi\rangle+\sum_{\beta=1}^{5}\langle\beta|h_Q|\beta\rangle. \quad (25)$$

$\langle 0|h_Q|0\rangle+\langle+|h_Q|+\rangle+\langle-|h_Q|-\rangle=0$, and again allowing the hole to "smear out," we see that

$$\langle\Phi_{+\pi}|h_Q|\Phi_{+\pi}\rangle=\langle+|h_Q|+\rangle, \quad (26)$$

with similar expressions for $\Phi_{0\pi}$ and $\Phi_{-\pi}$. $\langle j|h_Q|j\rangle$ can be directly evaluated using the wave functions (17). The expectation values of $q=(3\cos^2\theta-1)/r^3$ and $\eta=3\sin^2\theta\cos^2\phi/r^3$ are also given in (17). Recalling that $h_Q=qQ(1-R)(1+\eta^2/3)^{1/2}$, Eq. (24) indicates that

$$\Delta E_Q=\langle\Psi|h_Q|\Psi\rangle=(4/7)\langle r^{-3}\rangle Q(1-R)A^2|\langle d|p\rangle_\pi|^2\times|(B+3\lambda)^{-2}-B^{-2}|$$

$$=\text{const}|\langle d|p\rangle_\pi|^2\left[1-\left(1+\frac{3h\lambda}{B}\right)^{-2}\right]. \quad (27)$$

If $3h\lambda\ll B$, the expression in the brackets becomes $6h\lambda/B$. Moreover, since $h\approx\text{const}/b^3$, we can set (27) equal to

$$\Delta E_Q=\text{const}|\langle d|p\rangle_\pi|^2\lambda/b^3=\text{const}|\langle d|p\rangle_\pi|^2\lambda(V_0/V). \quad (28)$$

(Note that the larger $h\lambda$ is, with respect to B, the less dependent the quadrupole splitting is upon the distortion, i.e., if the splitting is large to begin with, only the ground state is expected to receive transferred electrons; if the splitting is small, the gradient will reflect the extent to which the various levels are populated.)

We can now take the values of E_Q shown in Fig. 2 and see what variation of λ with pressure is required by this model. At atmospheric pressure, $\Delta E_Q=0.78$ mm/sec, $b^3=43.4$ a.u., and $|\langle d|p\rangle_\pi|^2=3.03\times10^{-3}$ a.u. We have seen that $\cos^2\theta_0=0.3471$, so that $\lambda_0=0.0138$. Thus the constant in (28) is given by

$$\frac{(0.78\text{ mm/sec})(43.4\text{ a.u.})}{(3.03\text{ a.u.})(0.0138)}\times10^3=0.81\times10^6\text{ mm/sec}.$$

The change of θ required by this model is shown in Fig. 7 along with that corresponding to the point-charge model. It is seen that the behavior of θ with pressure is similar to that required by the point-charge model except that the maximum distortion occurs at lower pressure and the tendency towards higher symmetry at higher pressure is more pronounced. The actual behavior of θ versus P could be shown to lie somewhere above the lower of the two curves of Fig. 7, depending upon the relative strengths of the two effects, since the lower of these represents the extreme of a point-charge model while the upper represents only a transferred electron model, ignoring the contribution of a ligand-field gradient. Evaluation of the constants in Eqs. (4) and (27) indicate that the contribution due to covalency is of the order of 25% of that due to the distorted octahedron directly, but as indicated earlier, the absolute values for the Sternheimer and other factors are questionable. In any event, a composite model would, as does either extreme, require but a small variation in θ to account for the data.

[18] It should be mentioned that $|\xi_0|^2\langle\Phi_0|h_Q|\Phi_0\rangle$ represents the point charge gradient corrected for finite distribution of the electrons on the fluorides. At the moment we are not considering this term.

TABLE I. X-ray data for FeF_2.

Pressure (kbar)	a	c
0	4.697	3.309
27	4.68	3.24
58	4.66	3.18
100	4.64	3.11
133	4.63	3.09

TEMPERATURE DEPENDENCE

Figure 2 illustrates that K_3FeF_6 shows a quadrupole splitting at 143°K which is about 87% of the splitting at room temperature and that the pressure dependence of these splittings is about the same. This phenomenon can be accounted for in the covalent model by observing that the higher-lying T_{2g} levels are more easily populated by electron transfer at higher temperatures. In short, the thermal energy tends to randomize the distribution of transferred electrons, thus increasing the average symmetry and decreasing the gradient at the nucleus. A Boltzmann factor can be entered into the population probabilities. After evaluation of the matrix elements, Eq. (20) appears as

$$\Delta E_Q = \text{const}(2|a_{0\pi}|^2 - |a_{+\pi}|^2 - |a_{-\pi}|^2). \quad (29)$$

Assuming t_{2g}^+ and t_{2g}^- to lie at $E=T_1$ above t_{2g}^0, the right-hand side of (28) becomes

$$\text{const}\times\frac{2|a_{0\pi}|^2 - |a_{+\pi}|^2 e^{-T_1/T} - |a_{-\pi}|^2 e^{-T_1/T}}{1+e^{-T_1/T}+e^{-2T_1/T}}. \quad (30)$$

If, for the present purposes, we consider $|a_{0\pi}|^2 \approx |a_{+\pi}|^2 = |a_{-\pi}|^2$ and T_1 only slightly varying with pressure, there arises the temperature factor

$$g(T) = (1-e^{-T_1/T})/(1+2e^{-T_1/T}), \quad (31)$$

which implies that the quadrupole splitting will be smaller when experiments are done at higher temperatures. It turns out that the ratio $g(T')/g(T)$ is nearly independent of T_1 (and consequently, of pressure) for $0<T_1<500$°K and 300°K$<T$, $T'<1000$°K. Within these limits, $g(T')/g(T)$ is given by T/T'. Thus, for the K_3FeF_6 experiment,

$$g(T')/g(T) \approx 300\text{°K}/420\text{°K} = 0.72. \quad (32)$$

If 50% of the quadrupole splitting were due to the covalent contribution, the splitting would be expected to drop halfway to this value or to 0.86 of the original value upon heating from 300 to 420°K. This is because the ligand-field contribution has no provision for temperature-dependent behavior (aside from a negligible volumetric increase due to thermal expansion).

The results of this calculation are seen as convincing evidence that the covalent contribution makes up a significant fraction of the field gradient, since the observed splitting dropped to about 0.87 of the room-temperature value upon heating to 420°K.

FERROUS COMPOUND FeF_2

In this section, we shall examine the behavior of the quadrupole splitting of a ferrous salt, FeF_2, with pressure. Ferrous fluoride has the rutile structure with a tetragonal unit cell containing two formula units.[19] (See Fig. 8.) We use the previously published Mössbauer measurements and the lattice parameters presented in Table I.

Point-Charge Treatment

The environment of each iron is a distorted octahedron of six fluorines. In choosing the axes, we shall take the four equidistant fluorine sites at 2.12 Å to determine the x, y plane. The z axis thus passes through the two fluorine sites at 1.99 Å. Since the fluorines in the x, y plane form a rectangle rather than a square, it will be convenient to choose the x and y axes parallel to the sides of the rectangle with the x-axis coincident with the crystallographic c axis. This choice results in the d_{xy} and the $d_{3z^2-r^2}$ orbitals being of E_g symmetry and lying higher in energy than the T_{2g} since they are directed more or less toward the negative ligands. The x, y, and z axes are all rotation axes of order 2, which implies that they are the major axes of the EFG tensor at the origin. This also means that the d_{xy}, d_{yz}, and d_{zx} orbitals are eigenfunctions of the crystal field, but the lower azimuthal symmetry will allow some mixing between $d_{x^2-y^2}$ and $d_{3z^2-r^2}$. Therefore, we adopt

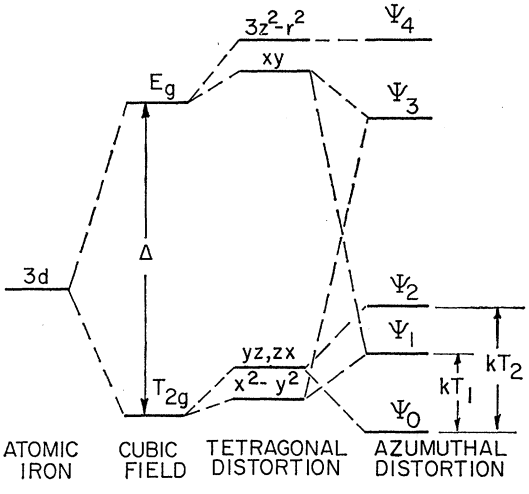

FIG. 9. Splitting of energy levels in FeF_2.

[19] J. W. Stout and S. A. Reed, J. Am. Chem. Soc. **76**, 5279 (1954).

TABLE II. Energies from the point-charge model.[a]

Configuration A	Pressure kbar 0	27	58	100	133
T_1	1300	1210	1120	1020	990
T_2	1150	1070	960	850	780
Configuration B					
T_1	1300	1180	1020	860	730
T_2	1150	990	820	630	480

[a] All energies in °K.

the following notation:

$$\begin{aligned} E_g:&\quad \Psi_4=\alpha|3z^2-r^2\rangle-\beta|x^2-y^2\rangle,\\ &\quad \Psi_3=|xy\rangle;\\ T_{2g}:&\quad \Psi_2=|zx\rangle,\\ &\quad \Psi_1=\alpha|x^2-y^2\rangle+\beta|3z^2-r^2\rangle,\\ &\quad \Psi_0=|yz\rangle, \end{aligned} \tag{33}$$

where $\alpha^2+\beta^2=1$. The subscripts are chosen so that the orbitals are arranged in the order of the energies as predicted by the point-charge field. (See Fig. 9.) Of the E_g orbitals, Ψ_4 is directed toward ligands lying at a lesser distance than those toward which Ψ_3 is directed. Thus, the E_g doublet is split and Ψ_4 lies higher. In the x, y plane, the ligands lie closer to the x axis as chosen, so that clearly $|zx\rangle$ lies above $|yz\rangle$. This leaves open to dispute the choice between Ψ_0 and Ψ_1 as the ground state. As Tinkham[20] has shown, a point-charge approximation leads to a ground state given by Ψ_0. Ganiel and Shtrikman[21] preferred to follow Abragam and Boutron[22] who, in their interpretation of Wertheim's Mössbauer data,[23,24] required, in their approximation, a ground state given by Ψ_1 to account for a measured value of η equal to $\frac{1}{3}$ at atmospheric pressure and 45°K, but equal to 0.4 at 4.2°K. By assuming a mixed ground state, it is possible to evaluate α and β. Both schemes will be presented here. The values of $\alpha=0.99$ and $\beta=0.11$ (from Ganiel and Shtrikman and the relation $\alpha^2+\beta^2=1$) will be taken for both presentations, since no better values are attainable from point-charge considerations. Knowledge of the exact value taken by β/α is not critical as long as the ratio is small, as it is expected to be since Δ, or $10Dq$, the splitting between the T_{2g} and E_g is of the order of 9000 cm^{-1} or 13 000°K.[25] Both treatments will ignore spin interaction.

The potential of the ligand point-charge field is expanded about the origin in spherical harmonics to give

$$V(\mathbf{r})=Zr^2\left(\frac{4\pi}{5}\right)^{1/2}\left[2\left(\frac{1}{b^3}-\frac{1}{p^3}\right)Y_2^0+\frac{\sqrt{6}}{p^3}\cos2\phi\,(Y_2^2+Y_2^{-2})\right]+Zr^4\left(\frac{4\pi}{9}\right)^{1/2}\left[\frac{1}{2}\left(\frac{4}{b^5}+\frac{3}{p^5}\right)Y_4^0\right.$$
$$\left.-\frac{\sqrt{10}}{2p^5}\cos2\phi\,(Y_4^2+Y_4^{-2})+\frac{\sqrt{70}}{4p^5}\cos4\phi\,(Y_4^4+Y_4^{-4})\right]+\text{6th and higher-order terms}. \tag{34}$$

Here b is the Fe-F distance along the z axis, while p is the Fe-F distance in the x, y plane. At atmospheric pressure, these are 1.99 and 2.12 Å, respectively. Z for the fluorines=1 and ϕ is the smallest, positive azimuthal co-ordinate of the fluorines in the x, y plane. Direct integration of the spherical-harmonic, triple-product integrals yields the energies E_2, E_1, and E_0.

$$\begin{pmatrix}\Psi_2\\ \Psi_1\\ \Psi_0\end{pmatrix}\Big|V(r)\Big|\begin{pmatrix}\Psi_2\\ \Psi_1\\ \Psi_0\end{pmatrix}=\begin{Bmatrix}E_2\\ E_1\\ E_0\end{Bmatrix}=K_2p^{-3}\left\{[(p/b)^3-1]\begin{bmatrix}1\\ -2(\alpha^2-\beta^2)\\ 1\end{bmatrix}+6\cos2\phi\begin{bmatrix}1\\ -2\alpha\beta/\sqrt{3}\\ 1\end{bmatrix}\right\}$$
$$+K_4p^{-5}\left\{[4(p/b)^5+3]\begin{bmatrix}-4\\ \alpha^2+6\beta^2\\ -4\end{bmatrix}-20\cos2\phi\begin{bmatrix}1\\ \alpha\beta/\sqrt{5}\\ -1\end{bmatrix}+35\cos4\phi\begin{bmatrix}0\\ \alpha^2\\ 0\end{bmatrix}\right\}, \tag{35}$$

where $K_2=(2/7)Z\langle r^2\rangle_{3d}$ and $K_4=(1/42)Z\langle r^4\rangle_{3d}$.

Table I gives the variation with pressure of the crystallographic a and c. Knowing these and the geometric relations

$$b=0.300a\sqrt{2},$$
$$(2p)^2=(0.400a\sqrt{2})^2+c^2$$

or

$$p=(a/2)[0.320+(c/a)^2]^{1/2}$$

and

$$\cos2\phi=c/2p,$$

the energies can be found as functions of K_2 and K_4.

In order to evaluate the K's, we will use Ganiel and Shtrikman's atmospheric values of T_1 and T_2 for the energy splittings indicated in Fig. 9. The particular order of the wave functions chosen by these authors had very little effect upon the numbers they ultimately got out, because of the way in which the orbitals

[20] M. Tinkham, Proc. Roy. Soc. (London) **A236**, 549 (1956).
[21] U. Ganiel and S. Shtrikman, Phys. Rev. **177**, 503 (1969).
[22] A. Abragam and F. Boutron, Compt. Rend. **252**, 2404 (1961).
[23] G. K. Wertheim, Phys. Rev. **121**, 63 (1961).
[24] G. K. Wertheim and D. N. E. Buchanan, Phys. Rev. **161**, 478 (1968).
[25] G. D. Jones, Phys. Rev. **155**, 259 (1967).

combine to produce the same gradient at the nucleus. That is, if only one orbital is occupied, the value of $q(1+\eta^2/3)^{1/2}$ is the same for any orbital (excluding a rather small effect from mixing it some Ψ_4). The configuration shown in Fig. 9 will be considered first. This arrangement of the levels will be referred to as "configuration A."

The ground state of configuration A is Ψ_0.

$$T_2=E_2-E_0=1300°\text{K}=(3.999K_2-0.827K_4)\times10^{-2},$$
$$T_1=E_1-E_0=1150°\text{K}=(0.794K_2+0.669K_4)\times10^{-2}. \quad (36)$$

The simultaneous solution of Eqs. (36) leads to values of $K_2=0.546\times10^5°\text{K}$ and $K_4=1.071\times10^5°\text{K}$. When these values are substituted back into (35), Table II results.

The energies of the T_{2g} levels decrease with compression as the crystal field grows. The splitting between them also decreases because as c/a decreases, the local symmetry about the iron increases.

In order to apply the thermal expression

$$V_{\mu\nu}(T)=(\sum_i[\langle\Psi_i|V_{\mu\nu}|\Psi_i\rangle e^{-E_i/kT}])/\sum_i e^{-E_i/kT}, \quad (37)$$

we need to calculate the matrix elements $\langle\Psi_i|q|\Psi_i\rangle$ and $\langle\Psi_i|q\eta|\Psi_i\rangle$, denoted q_{ii} and $(q\eta)_{ii}$. One obtains

$$q_{22}=q_{00}=(-2/7)\langle r^{-3}\rangle, \quad \eta_{22}=-\eta_{00}=3,$$
$$q_{11}=(+4/7)(\alpha^2-\beta^2)\langle r^{-3}\rangle, \quad \eta_{11}=2\sqrt{3}\alpha\beta/(\alpha^2-\beta^2), \quad (38)$$

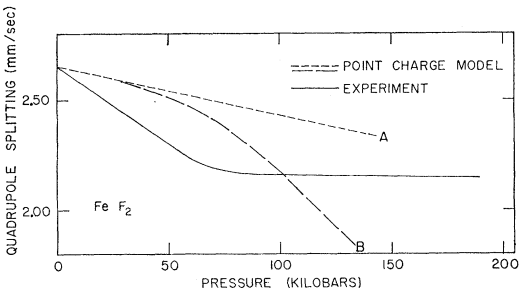

FIG. 10. Measured and calculated quadrupole splitting versus pressure—FeF_2.

whereupon Eq. (37) is evaluated as

$$\langle q\rangle=(2/7)\langle r^{-3}\rangle\frac{-1+2(\alpha^2-\beta^2)e^{-T_1/T}-e^{-T_2/T}}{1+e^{-T_1/T}+e^{-T_2/T}}$$

and

$$\langle q\eta\rangle=(2/7)\langle r^{-3}\rangle\frac{3-4\sqrt{3}\alpha\beta e^{-T_1/T}-3e^{-T_2/T}}{1+e^{-T_1/T}+e^{-T_2/T}}. \quad (39)$$

Again, we have the quadrupole splitting given by

$$\Delta E_Q=Q(1-R)[\langle q\rangle^2+\tfrac{1}{3}\langle q\eta\rangle^2]^{1/2}$$
$$=(4/7)\langle r^{-3}\rangle Q(1-R)f(T_1,T_2), \quad (40)$$

where the $f(T_1,T_2)$ for this configuration is

$$f(T_1,T_2)=\frac{[1+1.01e^{-2T_1/T}+e^{-2T_2/T}-1.36e^{-T_1/T}-e^{-T_2/T}-0.61^{-(T_1+T_2)/T}]^{1/2}}{1+e^{-T_1/T}+e^{-T_2/T}}. \quad (41)$$

Using T_1 and T_2 from Table II and $T=295°\text{K}$, $f(T_1,T_2)$ can be evaluated. Figure 10 depicts the observed curve,[1] as well as the above results.

In configuration B, the ground state is Ψ_1. This implies that the d_{yz}, d_{zx} doublet splits under the azimuthal distortion, but that both these levels still lie above the mixed state, primarily $d_{x^2-y^2}$. Accordingly,

$$T_2=E_2-E_1=1300°\text{K}=(3.205K_2-1.497K_4)\times10^{-2},$$
$$T_1=E_0-E_1=1150°\text{K}=(-0.794K_2-0.669K_4)\times10^{-2}. \quad (42)$$

These equations are directly analogous to Eqs. (36) and they, of course, imply new values for K_2 and K_4. $K_2=-0.256\times10^5°\text{K}$ and $K_4=-1.1416\times10^5°\text{K}$. The resulting values for T_1 and T_2 appear in Table II. Equations (39) now take a slightly different form, with the reassignment of the T_i. Taking this into account, the $f(T_1,T_2)$ of (40) configuration B is given by

$$f(T_1,T_2)=\frac{[1.01+e^{-2T_1/T}+e^{-2T_2/T}-1.36e^{-T_1/T}-0.61e^{-T_2/T}-e^{-(T_1+T_2)/T}]^{1/2}}{1+e^{-T_1/T}+e^{-T_2/T}}. \quad (43)$$

The predicted quadrupole splitting for this model also appear in Fig. 10. While the data do not permit one to select unequivocally the best model, Configuration A seems superior, as the curvature is better. More seriously, configuration B requires negative values of K_2 and K_4 which seems unreasonable.

Covalent Contributions

Although the contribution to the quadrupole splitting of ferrous compounds is expected to be small, it is interesting to note that its effect is negative, whereas in ferric compounds, it is positive. In FeF_2, where the

iron is surrounded by fluoride ligands, this contribution is expected to be especially small, since in the first part of this section, the covalency of the fluorine produced a gradient comparable to that arising directly from the distorted ligand field. The latter gradient is expected to be smaller than the gradient due to the valence electron by a factor of about $b^{-3}/\langle r^{-3}\rangle$, where b is the iron-fluorine distance (about 4 a.u.) and $\langle r^{-3}\rangle$ of the electron is about 5.1 a.u. according to Ingalls.[26] This is a factor of about 3×10^{-3}. Thus, the covalent contribution is expected to amount to only about 0.3% of the total quadrupole splitting in FeF_2.

The formalism of the theory directly follows that outlined for K_3FeF_6 above. When this is applied, and a value for $\alpha_{d\pi}$ of 0.05 a.u. is assumed,[27] the covalent contribution is about 0.25%.

[26] R. L. Ingalls, Ph.D. Thesis, Carnegie Institute of Technology, 1962 (unpublished).

[27] Hubbard *et al.* give values of $\alpha_{d\pi}$ equal to 0.03 and 0.07 for $KMnF_3$ and $KNiF_3$, respectively.

ACKNOWLEDGMENT

The authors wish to acknowledge the assistance of G. de Pasquali with the synthesis of the ferric compounds.

PHYSICAL REVIEW B VOLUME 1, NUMBER 4 15 FEBRUARY 1970

Crystallization and Instabilities in Highly Anharmonic Crystals*

GÜNTHER MEISSNER†
Laboratory of Atomic and Solid State Physics, Cornell University, Ithaca, New York 14850
(Received 17 June 1969)

A unified treatment of crystalline order and instabilities in highly anharmonic crystals at all temperatures is presented. This treatment is based on the study of singularities in the atomic-displacement correlation function or its Fourier transform (structure factor). As a result, it is rigorously shown that in the thermodynamic limit the mean-square fluctuations of the equilibrium position of a lattice particle are infinite in one and two dimensions at nonzero temperatures and in one dimension at *zero temperature*. This result, which is proved for an interacting many-body system without assuming the harmonic approximation, is obtained by using an exact Dyson equation for the displacement-response function. At finite temperatures, the demonstration of similar instabilities in a variety of condensed many-body systems of one and two dimensions is usually based on inequalities originally due to Bogoliubov. Since an analogous inequality can readily be extracted from the Dyson equation of the present approach, our method allows the extension of these results in anharmonic crystals to zero temperature. Finally, it is shown that additional dynamical information in this Dyson equality can be used to derive the relationship between elastic anomalies and sound absorption in the vicinity of critical points from the anomalous increase of the second derivative of the displacement-autocorrelation function.

I. INTRODUCTION

IN a number of physical systems, the traditional approach to lattice dynamics, that of expanding the interatomic potential in powers of atomic displacements, is entirely inadequate. Conspicuous examples are the so-called quantum crystals, such as the crystalline forms of the isotopes of helium, where the zero-point motions are large, or the paraelectrics of the $SrTiO_3$ family, where the polarizations are large. In particular, when applied to solid helium, the harmonic approximation yields a negative dynamical matrix and, therefore, imaginary phonon frequencies.[1] On the other hand, x-ray measurements show that these systems *do* form crystals with well-defined structures. For these reasons, a *microscopic* theory of such highly anharmonic crystals must specify a criterion for crystalline ordering which does not start from the harmonic approximation. Of a variety of choices available for selection as such a criterion, two are of particular interest. They are related to two different theoretical treatments—the single-particle and the collective picture—which have emerged for allowing the displacive motions of the particles in such systems to be large.[2]

In the single-particle picture, it has been shown[3] that long-range order in the crystalline phase may be attributed to a translational symmetry breaking statistical operator. This gives rise to nonvanishing Fourier components ρ_κ of the one-particle density for nonzero reciprocal lattice vectors $\boldsymbol{\kappa}$. The umklapp phonons, which are revealed as Bragg peaks in the scattering of x-rays, can then be obtained as the symmetry restoring collective

* Work supported by U. S. Atomic Energy Commission under Contract No. AT(30-1)-3699, Technical Report No. NYO-3699-39, and the Deutsche Forschungsgemeinschaft. A short account of this work was reported by G. Meissner, Bull. Am. Phys. Soc. 14, 367 (1969).

† On leave from the Max-Planck-Institut für Physik, München, Munich, Germany. Present address: Institut Max von Laue—Paul Langevin, München-Garching, Germany.

[1] F. W. de Wette and B. R. A. Nijboer, Phys. Letters **18**, 19 (1965).

[2] N. R. Werthamer, Am. J. Phys. **37**, 763 (1969). This paper gives a detailed review of the two different approaches to the theory of highly anharmonic crystals.

[3] G. Meissner, Z. Physik **205**, 249 (1967).